

Nanostructure evolution in joining of Al and Fe nanoparticles with femtosecond laser irradiation

Z. Jiao, H. Huang, L. Liu, A. Hu, W. Duley, P. He, and Y. Zhou

Citation: [Journal of Applied Physics](#) **115**, 134305 (2014); doi: 10.1063/1.4869656

View online: <http://dx.doi.org/10.1063/1.4869656>

View Table of Contents: <http://scitation.aip.org/content/aip/journal/jap/115/13?ver=pdfcov>

Published by the [AIP Publishing](#)

Articles you may be interested in

Densification behavior, microstructure evolution, and wear property of TiC nanoparticle reinforced AlSi10Mg bulk-form nanocomposites prepared by selective laser melting

[J. Laser Appl.](#) **27**, S17003 (2015); 10.2351/1.4870877

Slowing of femtosecond laser-generated nanoparticles in a background gas

[Appl. Phys. Lett.](#) **105**, 213108 (2014); 10.1063/1.4902878

Magnetic properties on the surface of FeAl stripes induced by nanosecond pulsed laser irradiation

[J. Appl. Phys.](#) **115**, 17B901 (2014); 10.1063/1.4862376

Facile synthesis of single-phase spherical α "-Fe₁₆N₂/Al₂O₃ core-shell nanoparticles via a gas-phase method

[J. Appl. Phys.](#) **113**, 164301 (2013); 10.1063/1.4798959




Formation of FePt nanoparticles by organometallic synthesis

[J. Appl. Phys.](#) **101**, 104313 (2007); 10.1063/1.2724330



AIP | Journal of Applied Physics

Meet The New Deputy Editors

	Christian Brosseau		Laurie McNeil		Simon Phillpot
---	---------------------------	---	----------------------	---	-----------------------

Nanostructure evolution in joining of Al and Fe nanoparticles with femtosecond laser irradiation

Z. Jiao,^{1,2} H. Huang,^{2,3} L. Liu,^{3,4} A. Hu,^{3,5} W. Duley,^{2,6} P. He,^{1,a)} and Y. Zhou^{2,3,a)}

¹State Key Laboratory of Advanced Welding Production Technology, Harbin Institute of Technology, Harbin 150001, China

²Centre for Advanced Materials Joining, University of Waterloo, Waterloo, Ontario N2L 3G1, Canada

³Department of Mechanical and Mechatronics Engineering, University of Waterloo, Waterloo, Ontario N2L 3G1, Canada

⁴Department of Mechanical Engineering, Tsinghua University, Beijing 100084, China

⁵Department of Mechanical, Aerospace, and Biomedical Engineering, University of Tennessee, Knoxville, Tennessee 37916, USA

⁶Department of Physics and Astronomy, University of Waterloo, Waterloo, Ontario N2L 3G1, Canada

(Received 12 February 2014; accepted 14 March 2014; published online 1 April 2014)

The joining of Al-Fe nanoparticles (NPs) by femtosecond (fs) laser irradiation is reported in this paper. Fe and Al NPs were deposited on a carbon film in vacuum via fs laser ablation. Particles were then exposed to multiple fs laser pulses at fluences between 0.5 and 1.3 mJ/cm². Transmission Electron Microscopy (TEM) and Electron Diffraction X-ray observations indicate that Al and Fe NPs bond to each other under these conditions. For comparison, bonding of Al to Al and Fe to Fe NPs was also investigated. The nanostructure, as observed using TEM, showed that individual Al NPs were monocrystalline while individual Fe NPs were polycrystalline prior to joining and that these structures are retained after the formation of Al-Al and Fe-Fe NPs. Al-Fe NPs produced by fs laser joining exhibited a mixed amorphous and crystalline phase at the interface. Bonding is suggested to originate from intermixing within a region of high field intensity between particles.

© 2014 AIP Publishing LLC. [<http://dx.doi.org/10.1063/1.4869656>]

I. INTRODUCTION

Recently, rapid progress in nanoscience and nanotechnology has generated a high demand for techniques that can be used for the joining of nanoscale building blocks to facilitate the assembly of systems having complex functionality.^{1,2} The joining of nanoparticles (NPs) is basic to this developing technology and is fundamental in the integration of nanoscale products. An important aspect of joining at the nano-scale is the maintenance of control over the melting depth in NPs.³ When two NPs are completely melted, the surface tension causes the two NPs to merge to form a larger particle.⁴ Irradiation with fs laser pulses minimizes bulk heating effects and offers new promise in the nanofabrication of novel nanodevices and multifunctional molecular systems.^{1,3} Since the fs laser pulse width is much shorter than the electron lattice thermal coupling time, excited electrons do not transfer energy to the lattice during the laser pulse. As a result, surface melting occurs and there is little heating or damage to the core of the particle. This property is ideal for welding of NPs.⁵ Huang *et al.*⁶ successfully joined Ag NPs in aqueous solution using fs laser irradiation, while Hu *et al.*⁷ joined Au NPs in solution by fs laser irradiation. However, no studies have focused on the joining of dissimilar metal NPs with ultrashort laser pulses.

The physical properties of Al and Fe, e.g., melting point, structure, and optical characteristics, are quite different from each other. Significantly, there are many existing and future

nanoscale applications involving Al-Fe systems. Al-Fe alloy nanopowders, which are self-protected by aluminum oxide, have outstanding stability compared to other alloys and thus have been widely used in environmental applications at high temperatures.⁸ Al-Fe alloys have also been of interest because of their excellent resistance to oxidation and sulfidation, which has led to many applications.⁹ Micron scale powders of Al-Fe alloys can be produced by ball milling, which results in the formation of an amorphous phase under non-equilibrium conditions.¹⁰ Aluminum alloys are the important materials in the manufacture of car bodies,¹¹ but there are a number of limitations inhibiting the widespread use of these alloys. For example, it has been found that it is often difficult to optimize weld strength and other weld characteristics when welding Al to steel because of the formation of brittle Al-Fe intermetallic phases.^{12,13} Accordingly, a fundamental understanding of the joining mechanism between Al and Fe can only be obtained from a detailed study of joining on the micro- and nano-scale. To date, there have been few reports of the composition and structure of Al-Fe joints over these scale lengths. This information is essential in the development of an overall model that can be used to describe the processes involved in the joining of Al and Fe.

Most previous studies have focused on the joining of NPs in aqueous solution using fs laser irradiation. While this is straightforward for Ag particles, Al and Fe NPs are easily oxidized,^{14,15} complicating the overall process. One way tackling this problem is to produce Al and Fe directly in vacuum by laser ablation of the parent metal. Pulsed laser deposition (PLD) has been widely used for the deposition of metal NPs in many applications.^{16,17} In the present

^{a)}Authors to whom correspondence should be addressed. Electronic addresses: hepeng@hit.edu.cn and nzhou@uwaterloo.ca

experiments, metal NPs have been deposited via PLD on a substrate in vacuum and characterized prior to joining.

In this work, we report the first study of fs laser-induced joining of Al and Fe NPs in vacuum. The nanostructure of the joints between particles is discussed in detail and a mechanism for the joining of these dissimilar metal NPs with fs radiation is proposed. Our findings show that joining is controlled by fs laser induced intermixing of Al and Fe atoms. The present results provide further insight into the processes involved in joining of dissimilar metallic NPs using fs laser irradiation.

II. EXPERIMENT

The experiments involved preparation and joining of NPs in vacuum with an fs laser system (1 kHz, 800 nm, Coherent, Inc.). The maximum pulse energy was 3.5 mJ at a pulse duration of 35 fs. NPs were first deposited on a ultrathin carbon film (400 mesh, <3 nm carbon film, copper transmission electron microscopy (TEM) grid, Ted Pella) in vacuum by separated laser ablation of Al (99.99%, Sigma) and Fe foil (99.99%, Sigma) at fluences of 165 mJ/cm² and 89 mJ/cm², respectively. The ablation time was 3 s (3000 pulses) for both materials. The resulting NPs were then exposed to fs laser irradiation for 5 s at fluences between 0.5 and 1.3 mJ/cm² to investigate the joining process. At these fluences, the diameter of the laser spot was around 1 cm, which covered the entire substrate so that all the particles on the substrate were exposed to laser radiation. To study the dissimilar materials' nanojoining, two continuing ablation were carried on with Fe and Al targets but deposited onto the same substrate. This resulted in a nanocomposite films with well mixed Fe and Al NPs. Ablation and irradiation of the deposited sample were carried out in vacuum at a base pressure of 10⁻⁶ Torr. A schematic of the experimental set up is shown in Fig. 1. High resolution TEM (HRTEM, JEOL 2010F) together with electron diffraction X-ray (EDX) was used to investigate the nanostructure and elemental distribution of the samples.

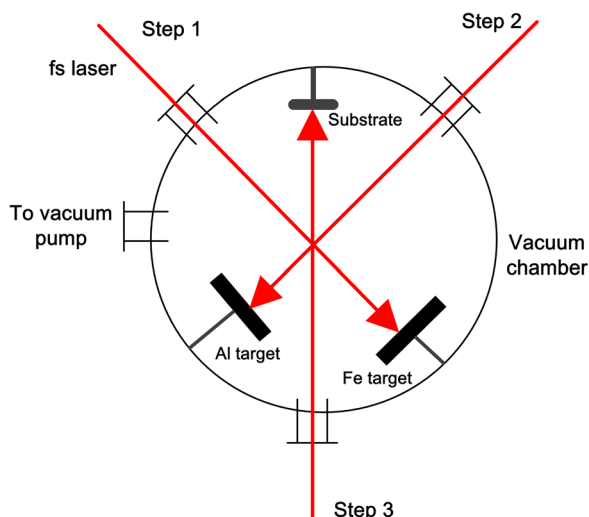


FIG. 1. Experimental configuration for the production and fs-laser joining of Al and Fe NPs in vacuum.

III. RESULTS AND DISCUSSION

A. Deposition of Al and Fe NPs

Initial experiments were carried out to ascertain the laser ablation conditions that yielded an optimum distribution of each type of NPs on the deposition surface. Figs. 2(a)–2(c) show the distributions of Al NPs produced at laser ablation fluences of 280, 165, and 89 mJ/cm², respectively. It was clear that ablation at high fluence (280 mJ/cm²) produced so many Al NPs that many overlapping particles were found, which could confuse investigation of the laser-induced joining phenomenon. At much lower laser ablation fluence (89 mJ/cm²), only a few Al NPs were detected on the substrate (Fig. 2(c)), which was also not ideal for a study of laser joining. For Fe NPs, laser ablation at fluences of 280 and 165 mJ/cm² also yielded excessively dense deposits with many overlapping NPs (Figs. 2(d) and 2(e)). After several trials, laser fluences of 165 mJ/cm² for Al and 89 mJ/cm² for Fe were found to produce well dispersed particles. Samples prepared under these conditions are shown in Figs. 2(b) and 2(f). The size of most Al and Fe NPs varied from 20 nm to 50 nm. The results show that laser fluence is the dominant parameter determining NP size and production rate.

B. Nanostructure of individual Al and Fe NPs

TEM scans were used to investigate the nanostructure of individual Al and Fe NPs after deposition and prior to irradiation. High resolution TEM images showed that the lattice planes in Al had constant orientation, indicating that individual Al NPs were monocrystalline (Fig. 3(a)). Similar scans showed that the orientation of lattice planes varied inside Fe NPs, showing that Fe NPs were polycrystalline (Fig. 3(b)). Lattice fringes in these images are marked with white lines.

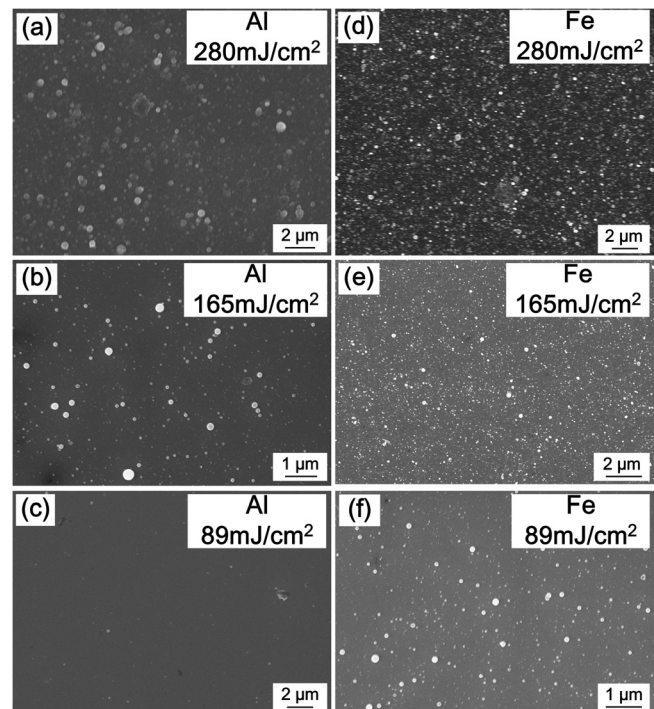


FIG. 2. SEM images of deposited Al and Fe NPs produced by laser ablation at fluences of 280, 165, and 89 mJ/cm². (a)–(c) Al NPs, (d)–(f) Fe NPs

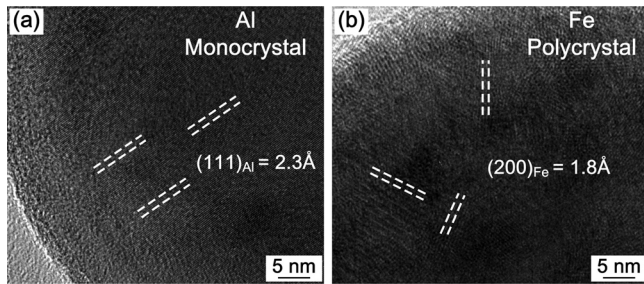


FIG. 3. High resolution TEM images of individual NPs prior to femtosecond laser irradiation. (a) Al NP and (b) Fe NP.

The measured lattice spacing for Al was $(111)_{\text{Al}} = 2.3 \text{ \AA}$ while that for Fe was $(111)_{\text{Fe}} = 1.8 \text{ \AA}$. Al and Fe exhibited distinct ablation responses under optimized conditions because of differences in fluence, ablation threshold, and material properties. Further investigation and detailed evidence are required to confirm the specific mechanism.

Fig. 4 shows high resolution TEM images of individual NPs after fs laser irradiation at a fluence of 1.3 mJ/cm^2 , which was the same condition that produced joining in mixed NP samples. It appeared that the nanostructure of Al remained monocrystalline while that of Fe was still polycrystalline. The measured lattice spacing for Al and Fe were also unchanged after fs laser irradiation. Although previous work has found that fs laser irradiation can induce microstructural changes in some materials,¹⁸ our results indicate that, due to the low laser fluence, the nanostructure of individual Al and Fe NPs were unaffected by irradiation.

C. Joining behavior of Al and Fe NPs

To study the joining of Al and Fe NPs, both types of particle were deposited on the same substrate. Fig. 5(a) shows the SEM image of a mixed Al/Fe sample after each component was deposited using the optimized laser ablation parameters. The distribution was such that individual particles can be distinguished without many overlapping NPs. The diameter of the NPs varied from 20 nm to 120 nm and almost all the NPs were spherical and isolated from other particles. However, after fs irradiation, many of these particles are seen to be joined to each other (Fig. 5(b)). The inset in Fig. 5(b) shows one of the joined Al-Fe NPs. The long-dashed circles indicate the original position of each NP. The gap between these two circles shows that two separate NPs become joined together after fs laser irradiation. The shape of the neck between the joined particles, as shown with the

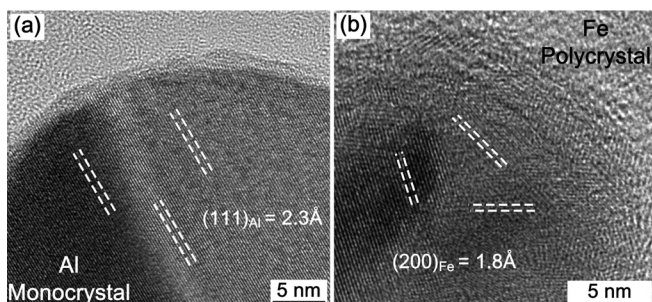


FIG. 4. High resolution TEM images of individual NPs after irradiation at 1.3 mJ/cm^2 . (a) Single Al NP and (b) Single Fe NP.

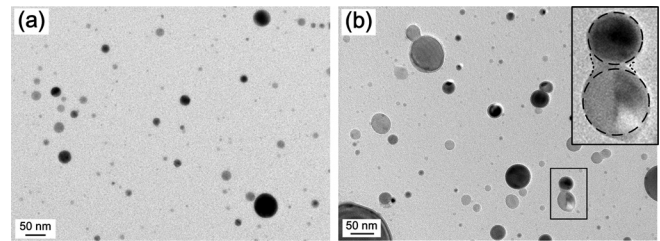


FIG. 5. SEM images of mixed Al and Fe NPs. (a) Before fs laser irradiation. (b) After fs laser irradiation at a fluence of 1.3 mJ/cm^2 . The inset shows a high magnification image of the highlighted area.

short-dashed lines, indicates that material from both particles has migrated into the gap during irradiation.

Before analyzing the structure of joined Al-Fe NPs produced by fs laser irradiation, it is useful to examine the structure in Al-Al and Fe-Fe NPs as shown in the insets in Fig. 6. Fig. 6(a) shows a high resolution image of the interface between Al-Al NPs and indicates that the nanostructure of each Al NP remains monocrystalline after fs laser irradiation. The dashed black line traces the Al-Al interface. The lattice orientation of both particles was seen to align in the same direction. Fig. 6(b) shows the nanostructure at the interface of a joined Fe-Fe NP after laser irradiation. The interface is traced by the black dashed line. Both particles retain their polycrystalline structure after irradiation and the measured lattice spacing was also unchanged. It was also apparent that, although there were different lattice orientations in each particle, the orientation across the interface was uniform in each particle. In previous research, Banfield *et al.*¹⁹ has reported that adjacent 2–3 nm particles tend to aggregate and rotate so that their nanostructures adopt parallel orientations in three dimensions. This phenomenon may be caused by particle collisions or by the short range interaction between adjacent surfaces.²⁰ From a thermodynamic point of view, this behavior can result in the reduction of surface free energy, which facilitated the joining process of NPs of uniform composition. This is similar to joining of silver NPs where the particles rotate to align to each other.²¹

A TEM image of an Al-Fe NP joined by exposure to fs laser irradiation is shown in Fig. 7(a). It can be seen from Figs. 7(b) and 7(c) that the interior of the Al NP was still monocrystalline while the interior of the Fe NP was polycrystalline after joining. Therefore, both Al and Fe NPs

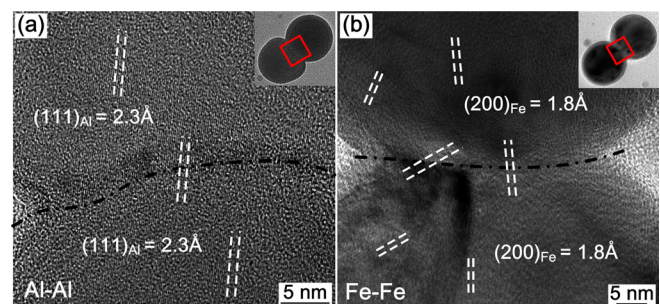


FIG. 6. TEM images of joined NPs with homogeneous composition. (a) High resolution image of the Al-Al interface. (b) High resolution image of the Fe-Fe interface. In each case, the black dashed line traces the interface. Insets show a TEM image of the overall morphology. The red square indicates the area shown in the high resolution images.

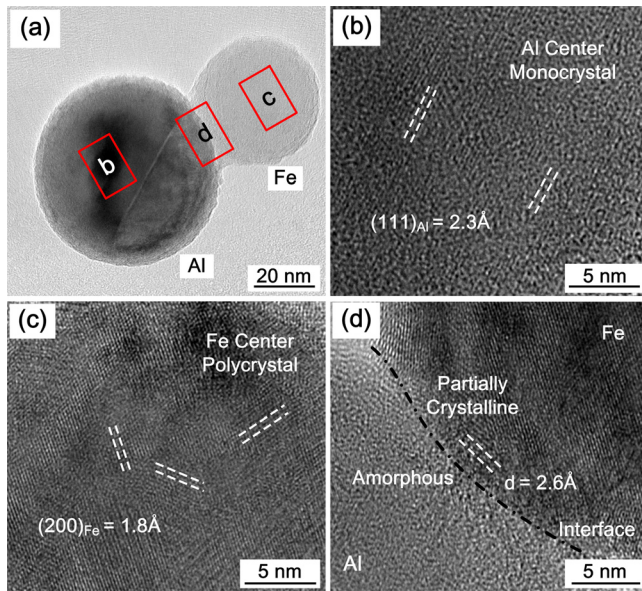


FIG. 7. High resolution TEM images of Al-Fe NPs joined by exposure to fs laser radiation. (a) Morphology of joined Al-Fe NPs. The letters show the corresponding high resolution image and the red squares indicate the corresponding area. (b)–(d) High resolution TEM image of the corresponding area.

retained their initial nanostructure after joining. However, the nanostructure was different within the Al-Fe interface (Fig. 7(d)). An amorphous phase was found near the interface, particularly on the side toward the Al particle. The interface region exhibited a mixed amorphous and crystalline

structure near the Fe particle, but the nanostructure became fully crystalline in the region closer to the center of the Fe particle.

Fig. 8(b) shows line scan EDX results across a joined Al-Fe NP having the morphology shown in Fig. 8(a). It shows that a mixed layer, with thickness around 10 nm, was found at the interface. The layer is also confirmed by the spot scan data, as shown in Fig. 8(c). The resolution of the EDX spot scan was around 1 nm and the spot locations were as indicated by the numbers in Fig. 8(a).

In Sec. III B, it was shown that the nanostructure of Al and Fe remained the same after femtosecond laser irradiation of individual NPs. This was also observed in Al-Al and Fe-Fe NPs joined by exposure to fs radiation and the nanostructure within the interface remained crystalline, so it is evident that, in joined Al-Fe NPs, the amorphous phase was not simply caused by exposure to femtosecond laser radiation. In addition, the lattice spacing of the partially crystalline structure near the interface was 2.6 Å (Fig. 7(d)), which was different from that of either pure Al or Fe. We believe that this difference can be attributed to the formation of an Al-Fe alloy. The amorphous and partially crystalline phases can be formed due to the atomic intermixing properties of these two dissimilar materials. Garcia-Navarro *et al.*²² have discussed the damage caused by femtosecond laser irradiation using a two-step phenomenological scheme. The results indicate that the first stage involves strong electronic excitation leading to the formation of a high density electron-hole plasma, while the second stage involves the relaxation of the stored

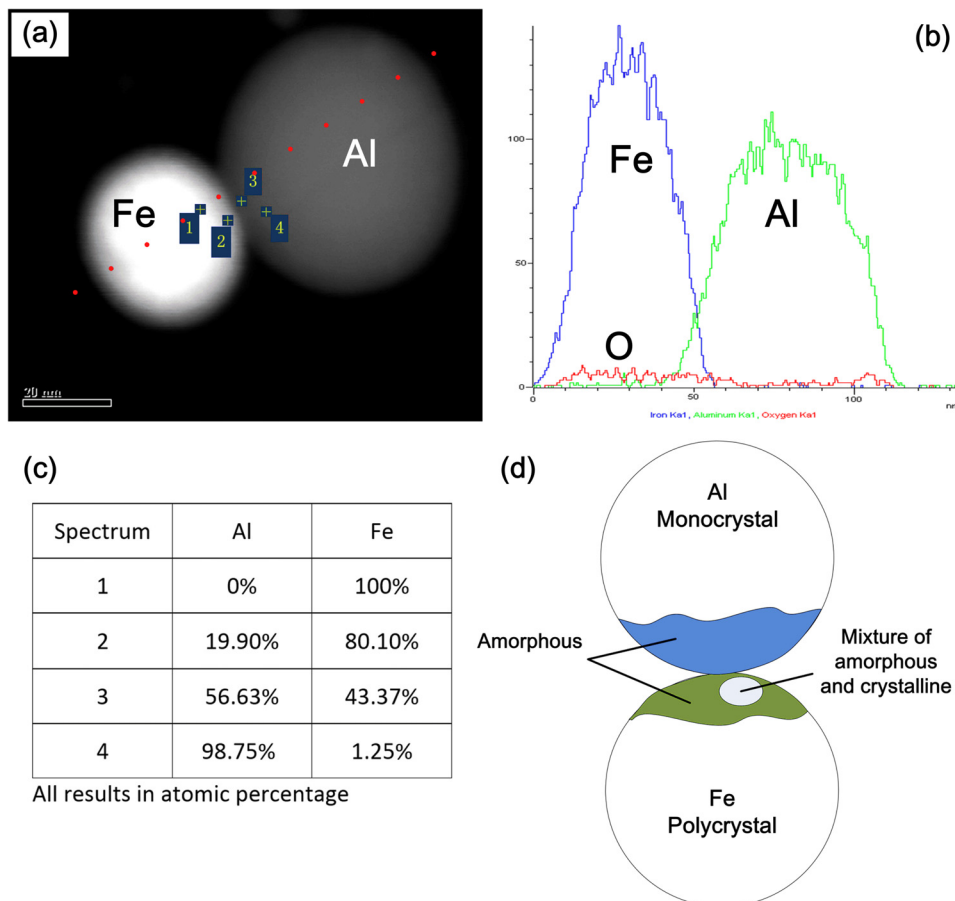


FIG. 8. (a) Morphology of joined Al-Fe NPs. Numbers indicate the locations of the EDX spot scans. The red line shows the line scan position. (b) EDX results of joined Al-Fe NPs. (c) EDX spot scan results expressed as atomic percentage. (d) A schematic representation of nanostructure in joined Al-Fe NPs.

excitation energy of electrons by transfer to the lattice resulting in bond breaking, and defect generation. Both effects yield a weakening of bonding between surface atoms, resulting in a softening of the lattice structure within the surface. The softened surface is distinct from a normal molten phase because the effective temperature has not reached the melting point for either type of particle.²³ The overall neck structure is very similar to that seen in the microwave²⁴ and plasma²⁵ sintering of metal nanopowders where it has been associated with surface diffusion.²⁵ In the fs interaction, the electric field is concentrated in the gap between adjacent particles resulting in the emission of electrons from these "hot-spots." These energetic electrons are accompanied by spallation as electrons emitted from one particle impact on the other. Heating arising from electron impact results in a softening of the lattice in each particle at the interface.⁶ Atomic mixing in the interface and the formation of a necking bridge can then be attributed to a combination of spallation from both particles, together with diffusion of both Fe and Al into the bridging region.

Liu²⁶ has noted that such intermixing is a non-equilibrium process, which produces a mixing layer in a highly disordered and energetic state. After intermixing has ended, the mixture relaxes towards an equilibrium state, which is a function of the thermodynamic properties of the system. After fs excitation, this relaxation proceeds over a timescale measured in picosecond, which is much too rapid to allow the mixture to reach the equilibrium state. As a consequence, relaxation usually terminates at some intermediate state characterized by metastable crystalline or amorphous phases. Calculations of enthalpy as a function of composition in the Al-Fe system²⁷ using the Miedema model²⁸ indicates that, when the atomic percentage of Fe is between 30% and 60%, the mixture tends to form an amorphous low enthalpy phase. When the proportion of Fe is between 10%–30% or 60%–90%, the system tends to form a mixture of amorphous and solid solutions, and when the proportion of Fe is <10% or >90%, the system exists as a solid solution. From the TEM results, it appears that the nanostructure of the interface is amorphous at the location of spot 3 (Figure 8). A mixture of amorphous and crystalline structure was found at location of spot 2 near the interface inside the Fe particle. We conclude that elemental compositions at the locations of these spots, corresponding to different nanostructures, are in good agreement with the Miedema model.²⁸ The Miedema theory is then consistent the detection of an amorphous structure in the interface between Al-Fe NPs as well as the existence of a localized mixture of amorphous and crystal phases. The overall nanostructure in joined Al-Fe NPs is summarized in Fig. 8(d). This study of joining Al-Fe NPs yields further insight into mechanisms involved in joining of dissimilar materials in nano-scale systems and indicates that nanojoining induced by fs laser radiation may have a number of practical applications in the generation of novel nanostructures.

IV. CONCLUSIONS

Al and Fe NPs have been deposited on a substrate in vacuum by fs laser ablation. Joining of Al and Fe NPs was

then carried out by irradiation of the mixed sample with low fluence fs laser pulses. The nanostructure and joining mechanism of Al and Fe have been investigated. The results showed that the nanostructure of Al NPs was monocrystalline after deposition, while that of Fe NPs was polycrystalline. These structures were retained after fs irradiation at fluences of 1.3 mJ/cm². Al-Al and Fe-Fe NPs were found to exhibit uniform lattice orientation after fs laser irradiation, and the nanostructure in the interface was the same as that of the individual NPs. In mixed samples, study of fs laser induced joining in Al-Fe NPs shows that the interface contains a mixture of amorphous and crystalline phases. Intermixing of Al and Fe in the region between the particles arises from electron heating of material on both sides of the interface together with diffusion and lattice softening. The composition of the amorphous and crystalline phases is in good agreement with the Miedema model.

ACKNOWLEDGMENTS

Financial support of National Sciences and Engineering Research Council (NSERC) and State Scholarship Fund of China (Grant No. 201206120144) are gratefully acknowledged. The authors would like to thank Ph.D. candidate Peng Peng and Dr. Mugunthan Sivayoganathan from Centre for Advanced Materials Joining, University of Waterloo, for valuable discussions. The authors thank Ms. Carmen Andrei from the Canadian Centre for Electron Microscopy, McMaster University for help with TEM operation.

- ¹Y. Zhou and A. Hu, *Open Surf. Sci. J.* **3**, 32 (2011).
- ²S. W. Guo, *Nanoscale* **2**, 2521 (2010).
- ³A. Hu, Y. Zhou, and W. W. Duley, *Open Surf. Sci. J.* **3**, 42 (2011).
- ⁴J. K. Chen and J. Q. Qui, *J. Nanopart. Res.* **14**, 942 (2012).
- ⁵D. von der Linde, K. Sokolowski-Tinten, and J. Bialkowski, *Appl. Surf. Sci.* **109**, 1 (1997).
- ⁶H. Huang, L. Liu, P. Peng, A. Hu, W. W. Duley, and Y. Zhou, *J. Appl. Phys.* **112**, 123519 (2012).
- ⁷A. Hu, P. Peng, H. Alarifi, X. Y. Zhang, and J. Y. Guo, *J. Laser Appl.* **24**, 042001 (2012).
- ⁸J. Y. Yun, H. M. Lee, S. Y. Choi, S. Yang, D. W. Lee, Y. J. Kim, and B. K. Kim, *Mater. Trans.* **52**, 250 (2011).
- ⁹S. C. Deevi, V. K. Sikkat, and C. T. Liu, *Prog. Mater. Sci.* **42**, 177 (1997).
- ¹⁰M. Krasnowski and T. Kulik, *Mater. Chem. Phys.* **116**, 631 (2009).
- ¹¹M. J. Zhang, G. Y. Chen, Y. Zhang, and K. R. Wu, *Mater. Des.* **45**, 24 (2013).
- ¹²H. Dong, L. Yang, C. Dong, and S. Kou, *Mater. Sci. Eng., A* **534**, 424 (2012).
- ¹³M. J. Torkamany, S. Tahamtan, and J. Sabbaghzadeh, *Mater. Des.* **31**, 458 (2010).
- ¹⁴T. J. Foley, C. E. Johnson, and K. T. Higa, *Chem. Mater.* **17**, 4086 (2005).
- ¹⁵X. Q. Li and W. X. Zhang, *Langmuir* **22**, 4638 (2006).
- ¹⁶N. R. Agarwala, F. Nerib, S. Trussoc, A. Lucottia, and P. M. Ossi, *Appl. Surf. Sci.* **258**, 9148 (2012).
- ¹⁷F. Gamez, A. Plaza-Reyes, P. Hurtado, E. Guillen, J. A. Anta, B. Martinez-Haya, S. Perez, M. Sanz, and M. Castillejo, *J. Phys. Chem. C* **114**, 17409 (2010).
- ¹⁸G. Zhang, D. Gu, X. Jiang, Q. Chen, and F. Gan, *Solid State Commun.* **133**, 209 (2005).
- ¹⁹J. F. Banfield, S. A. Welch, H. Zhang, T. T. Ebert, and R. L. Penn, *Science* **289**, 751 (2000).
- ²⁰J. Fang, X. Ma, H. Cai, X. Song, and B. Ding, *Nanotechnology* **17**, 5841 (2006).
- ²¹E. Marzbanrad, A. Hu, B. Zhao, and Y. Zhou, *J. Phys. Chem. C* **117**, 16665 (2013).
- ²²A. Garcia-Navarro, F. Agullo-Lopez, J. Olivares, J. Lamela, and F. Jaque, *J. Appl. Phys.* **103**, 093540 (2008).

²³J. A. Vanvechten, R. Tsu, and F. W. Saris, *Phys. Lett. A* **74**, 422 (1979).

²⁴D. Demirskyi, D. Agrawal, and A. Ragulya, *Scr. Mater.* **66**, 323 (2012).

²⁵Y. Q. Fu, C. Shearwood, B. Xu, L. G. Yu, and K. A. Khor, *Nanotechnology* **21**, 115707 (2010).

²⁶B. X. Liu and O. Jin, *Phys. Status Solidi A* **161**, 3 (1997).

²⁷D. K. Mukhopadhyay, C. Suryanarayana, and F. H. (Sam) Froes, *Metall. Mater. Trans. A* **26**, 1939 (1995).

²⁸A. K. Niessen, F. R. de Boer, R. Boom, P. F. de Chatel, W. C. M. Mattens, and A. R. Miedema, *CALPHAD: Comput. Coupling Phase Diagrams Thermochem.* **7**, 51 (1983).